RASĀYAN *J. Chem.*
Vol. 18 | No. 4 |2020-2029| October-December | 2025
ISSN: 0974-1496 | e-ISSN: 0976-0083 | CODEN: RJCABP
http://www.rasayanjournal.com
http://www.rasayanjournal.co.in

COAL-DERIVED GRAPHENE@POLIANILIN-ZINC OXIDE HYBRID NANOCOMPOSITE: A NEW MATERIAL WITH HIGH PERFORMANCE FOR PHOTOCATALYTIC APPLICATIONS

V. Purwandari[1,2], Marpongahtun[3,✉], Isnaeni [4], R. Goei[2,6], M. Harahap[2,5] and H. Syapitri[1]

[1]Department of Chemistry, University of Sari Mutiara Indonesia,
Jalan Kapten Muslim No. 79, Medan 20124, Indonesia
[2]Low Carbon Study Center, Universitas Sari Mutiara Indonesia,
Jalan Kapten Muslim No. 79, Medan 20124, Indonesia
[3]Universitas Sumatera Utara, Medan, 20155, Indonesia
[4]Photonics Research Center, National Research and Innovation Agency, Indonesia
[5]Politeknik Negeri Medan, Medan, 20155, Indonesia
[6]School of Materials Science and Engineering, Nanyang Technological University, Singapore
✉Corresponding author: marpongahtun@usu.ac.id

ABSTRACT

This study reports the synthesis of graphene (Gc) and a graphene@polyaniline-zinc oxide (Gc@PANI-ZnO) hybrid nanocomposite for methylene blue (MB) degradation. GC was synthesized from sub-bituminous coal from South Sumatera, Indonesia, using ultrasonication. Zinc oxide (ZnO) nanoparticles were prepared inside an autoclave with a Teflon lining at 180 °C for 6 h. Gc was then encapsulated with PANI through in-situ polymerization, followed by ZnO addition to enhance photocatalytic performance. The final Gc@PANI-ZnO nanocomposite was synthesized in a hydrothermal vessel with a Teflon lining and processed at 180 °C for 12 h. Characterization using TEM, SEM, XRD, and FT-IR confirmed the catalyst's structure and morphology. The Gc@PANI-ZnO catalyst achieved over 90% photocatalytic efficiency in less than 30 min under a 500-watt halogen lamp. The high efficiency was attributed to Gc's thermal conductivity (9.5×10^2 W/mK), enhancing electron transfer, while PANI improved dye adsorption and light absorption. ZnO enhanced the optical absorption spectrum and inhibited electron-hole recombination. This hybrid nanocomposite removed over 95% of MB in under 30 min and could be reused thrice, demonstrating excellent photocatalytic efficiency and stability for wastewater treatment applications.

Keywords: Coal, Graphene, Photocatalyst, Nanocomposite, Encapsulation.

RASĀYAN *J. Chem.*, Vol. 18, No. 4, 2025

INTRODUCTION

During fabrication, chemical industries involved in food, pharmaceuticals, plastics, paints, cloth, fiber, and farming make use of various chemicals, including organic dyes.[1] These compounds exhibit chemical stability and are resistant to decomposition.[2] Moreover, they pose a risk towards such surroundings as well as mankind's well-being when dissolved within fluid at concentrations of 1 mg/L or higher.[3,4] Methylene blue ($C_{16}H_{18}CN_3SCl$) (MB) is a cationic and predominantly used heterocyclic aromatic compound in the industry as a colouring agent. Water quality declines when contaminated with MB to cause dermis and optic organ irritation and interfere with renal organ, hepatic organ, cerebrum, genital system, and central neurological network.[5,6] The photocatalytic process that harnesses light energy to stimulate chemical reactions has become a promising technology for various environmental and energy applications.[7,8] Manufacturing effective and durable photocatalytic materials is critical to improving the overall application efficiency.[7,9] Lately, Graphene-related nanocomposites have attracted significant interest due to their distinctive properties and promising potential for diverse applications.[10-12] Among nanocomposite materials using graphene (G), Nanocomposite substance combines the advantages of G, PANI, and TiO to create a synergistic effect that enhances photocatalytic activity and stability.[13,14] G is an allotrope of carbon with a two-dimensional structure.[15,16] This material has a large surface area, high mechanical and electrical

http://doi.org/10.31788/RJC.2025.1839288

conductivity,[17] and outstanding optical properties.[18] The remarkable characteristics of G render it an ideal material for photocatalysis.[19] Integrating G into PANI,[20] a conductive polymer with good stability and redox properties,[21] encapsulating G in PANI (G@PANI) offers increased separation and charge transfer, thereby increasing photocatalytic efficiency.[22] A semiconductor material with a wide energy gap, namely ZnO, is known to have photocatalytic properties with high stability,[23] low toxicity,[24] and the ability to adjust band energy,[25] making it suitable for various photocatalytic applications. Adding ZnO to the G@PANI nanocomposite further enhances the photocatalytic activity because apart from acting as a co-catalyst.[26] ZnO also facilitates charge transfer processes and promotes the formation of reactive species.[27] Muhammad, F., K, *et al.* designed TiO_2@CeO_2 and CeO_2@TiO_2 layered hybrid structures utilizing Gc for applications in photocatalysis and cytotoxicity.[28] Zhang M *et al*., reported that composite photocatalysts of ZSM-5/$Bi_4O_5Br_2$ exhibit significant potential as highly effective photocatalysts for the degradation of rhodamine B. The MoS_2/g-C_3N_4 (MSC) nanocomposite was rapidly synthesized in just 30 min using a one-step microwave-assisted method. This approach resulted in a low recombination rate and an energy separation of 1.7 eV, making it highly effective for visible-light degradation with an efficiency of 98.7% and reusability for 5 cycles. This nanocomposite holds great potential for wastewater treatment applications.[29] Inorganic 2D nanosheets for photocatalytic CO_2 reduction are also discussed.[30] A material with nanosized structures has excellent properties not only in high-efficiency filter media but also in functionalizing surfaces through polymer chemistry, blending, and nanofiller incorporation.[31,32] This study reports on the synthesis of Gc from sub-bituminous coal obtained from South Sumatera, Indonesia. This is the first study to utilize the sample as a precursor of Gc. The GC is extracted by a simple ultrasonication method and is inexpensive. After that, Gc@PANI-ZnO hybrid nanocomposites are prepared for photocatalyst material. Gc@PANI-ZnO hybrid nanocomposites have unique structures and a broad surface area to enhance light absorption efficiency. The interaction between the constituent components (Gc, PANI, and ZnO) improves the process of separation and transport of charge carriers generated by light, as well as minimizes damage due to recombination. Gc@PANI-ZnO nanocomposite also shows excellent stability, reusability, and degradation resistance; hence, this material can be relied upon for long-term performance. The high performance of the Gc@PANI-ZnO nanocomposite hybrid makes it an attractive material that is applicable to diverse photocatalytic uses, including water treatment, air pollution mitigation, and solar fuel generation. This Gc@PANI-ZnO photocatalyst has extraordinary stability, which allows the decomposition of organic contaminants to be faster, more efficient, and can be reused, thereby reducing the cost and environmental impact of the entire photocatalytic process.

EXPERIMENTAL

Materials

GC was synthesized from sub-bituminous coal obtained from South Sumatera, Indonesia. All chemicals used in the experiments were of analytical quality and utilized as received, devoid of additional refinement. Every chemical used in this study was obtained from Sigma Aldrich - Indonesia. Each prepared solution was formulated using distilled water.

General Procedure

GC was produced from the exfoliation process of sub-bituminous coal by a multi-stage ultrasonication technique. Then, graphene/polyaniline encapsulation was carried out by the in situ polymerization technique. Followed by the addition of ZnO by the hydrothermal method. Testing the effectiveness of MB color degradation was carried out using a 500-watt halogen lamp.

Preparation of Graphene from Coal (Gc)

A total of 2 g of coal powder (C) was mixed with 200 mL of isopropyl alcohol and stirred for 90 s using a magnetic mixer at a speed of 400 revolutions per minute. The mixture was then ultrasonicated using an ultrasonication probe model B-One Ultrasonic cleaner BUC 100 L, 220 VAC/50 Hz for 30 min at 28 kHz. Ultrasonication was repeated until a stable suspension (±10x) was obtained. The Gc suspension was passed through a Whatman 42 filter paper to remove larger particles. This filtrate was then heated to remove moisture at 85-90 °C for 6 h, then kept in a dry container for future use. The graphical representation of the synthesis of C to Gc with the ultrasonic technique is presented in Fig.-1.

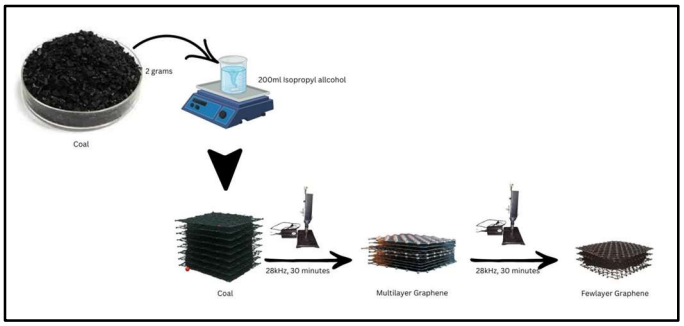

Fig.-1: Schematic of the Synthesis of Coal to Graphene with the Ultrasonic Technique

Encapsulation of Gc with PANI (Gc@PANI)

A total of 0.46 mL of aniline was dispersed in 50 mL of 1.0 N HCl within a triple-neck spherical flask, then 50 mg of Gc was added. The solution was soaked for 3 h, followed by adding 1.466 g comprising $(NH_4)_2S_2O_8$ (APS), and dispersed into 50 cc containing 1.0 N Hydrochloric acid. The APS solution was gradually introduced into the aniline solution, drop by drop. There was a change from semi-transparent to a blackish-green gel. The reaction was allowed to proceed over 24 h at 5 degrees centigrade. In the subsequent stage, it became separated through filtration, rinsed multiple times with distilled water, and then followed by methanol. The green-black precipitate was collected and dried in a heated chamber at 50 degrees centigrade for 24 h.

Manufacturing of Gc@PANI-ZnO Nano-hybrid material.

ZnO nanoparticles were combined with Gc@PANI powder in a 1:1 ratio, followed by the addition of 50 mL of purified fluid. NH_4OH was introduced to regulate the solution's pH to 9. The solution underwent continuous stirring at 400 rpm for 30 min, then was subjected to sonication at 28 kHz for 15 min. That mixture experienced placement inside the reactor and was exposed to heat at 180 degrees centigrade for 12 h. The same procedure was repeated for ZnO: Gc@PANI ratio 3:1. Diagram of Gc@PANI-ZnO nanocomposite preparation is illustrated in Fig.-2.

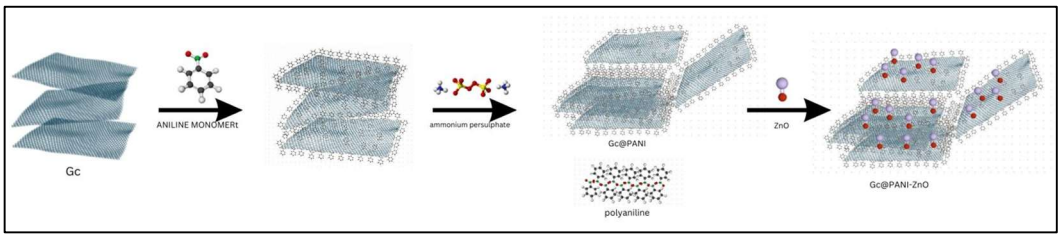

Fig.-2: Schematic of Gc@PANI-ZnO Nanocomposite Preparation

Catalyst Activity and Durability

The light-induced catalytic efficiency regarding Gc@PANI-ZnO was assessed by adding 30 mg of catalyst to 100 mL of a 5 mg/L MB solution. These blends were subsequently mixed for 30 min and followed by ultrasonication for 5 min. That mixture was placed under a 500-watt halogen lamp while being continuously stirred. Then pipette 5 mL of solution for the first 15 min, the second, and so on. Such a compound was subsequently separated using centrifugal force at 6000 rpm for about 15 min, followed by filtration to eliminate the catalyst before analysis. Variation in absorbance was measured using a UV-Vis analyzer.
This catalyst breakdown effectiveness is determined using eqn.-1 below:

$$\text{Decolorization efficiency} = (A_o\text{-}At)/A_o \times 100\% \quad (1)$$

A_o refers to the absorbance measured before irradiation, and A_t represents the absorbance at a given time t after the photocatalytic reaction.
The stability and durability of the synthesized Gc@PANI-ZnO nanocomposite hybrid were tested by thoroughly washing the photocatalyst for each cycle with distillate water and acetone. The photocatalyst is then dried at 90 °C for use in the next cycle.

Detection Method

The structural form was experienced analysis using a transmission electron microscope (TEM) on a Jeol 2100F using an applied electric potential of 80 kV. Field emission scanning electron microscopy (SEM) images were acquired using a Jeol 7600F equipped with EDX, functioning at an applied electric potential of 20 V. Crystalline configurations regarding the specimens were analyzed with a Shimadzu X-ray diffraction (XRD) 6000. XRD patterns were captured spanning 10–80 degrees, with a scan step size of 0.02 degrees and a step duration of 2° per minute. Infrared spectral analysis for each specimen was performed using a Perkin Elmer Frontier, scanning across 4,000–400 cm¹.

RESULTS AND DISCUSSION

Gc produced from sub-bituminous coal by a multi-stage ultrasonication method is used as filler material in catalysts (Fig.-1). The multi-stage process, a physical stage, was expected to be able to reduce the percentage of ashes in the sample. As discussed in a previous study, ash in Gc could be removed in subsequent stages of the process. In this study, the compositional analysis of the raw material has been presented in Table 1. Gc remains encapsulated by PANI to improve the stability and performance of Gc in catalytic systems. By adding ZnO to the catalyst, it can absorb light and generate more electron holes, which is important for photocatalytic reactions (Fig.-2). XRD pattern and FTIR spectra of samples are displayed in Fig.-3, while SEM, SEM MAPS, and TEM images are displayed in Fig.-4.

Table-1: Proximate Analysis of Sub-Bituminous Coal from South Sumatera

Proximate (% adb)			
Moisture	Volatile Matter	Ash	Fixed Carbon
8.19	46.00	2.10	43.71

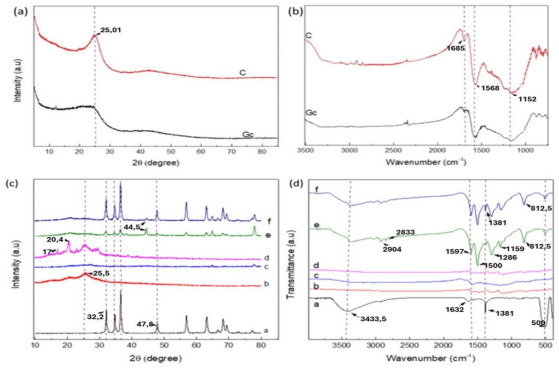

Fig.-3: (a) XRD C and Gc Patterns; (b) FTIR Spectra of C and Gc; (c) XRD Pattern and (d) FTIR Spectra of a) ZnO; b) PANI; c) Gc; d) Gc@PANI; e) Gc@PANI-ZnO-1; f) Gc@PANI-ZnO-3;

From Fig.-3 (a), it can be seen that there has been a change in the width of the peak from C to a lower and wider peak, which illustrates that there has been exfoliation of the C into graphite sheets with a varying number of layers.[33] According to XRD data and estimations derived from the Scherrer equation:[34]

$$D = (k.\lambda)/(\beta.\text{Cos }\theta) \quad (2)$$

The crystalline particle size regarding Gc derived from coal ultrasonication was measured at 27.8 nm, featuring an interlayer distance of 0.36 nm. This delicate configuration has been confirmed by the specified Gc Transmission Electron Microscopy (TEM) image. FTIR spectra (Fig.-3b) show a change at the peak of 1695 cm^{-1}; the reduced intensity of the carbonyl group (C=O) peak[35] in the repeated ultrasonication process of C. The XRD pattern of ZnO, 3(c) pattern a) shows the peak that is generally present in ZnO compounds, namely the highest peak at a diffraction angle of 2θ around 36°, followed by a peak of 2θ around 32° and 34°.[36] This ZnO diffraction pattern is reported to have good optical characteristics and is suitable for sensors with high humidity efficiency.[37] The XRD pattern for PANI, b) has several broad reflection peaks, one at a diffraction angle of 2θ around 25.5°, and the distance between layers (d) is 0.35 Å. In comparison, the diffraction pattern of Gc shows a very wide peak at the diffraction angle of 2θ is about 27°.[20] Synthesis of Gc@PANI, d) it was seen that there was a significant change in the diffraction pattern, indicating an

interaction that occurred in the aniline polymerization in situ process carried out on the surface of the Gc sheet. The formation of diffraction angle peaks 2θ around 17° and 20° indicates that Gc also follows the oxidative polymerization process from PANI. The diffraction patterns e) and f) are diffraction hybrid composites of Gc@PANI-ZnO-1 and Gc@PANI-ZnO-3. The results of the XRD analysis on these two samples showed that Gc@PANI-ZnO-1 was more compatible than Gc@PANI-ZnO-3. Even though the diffraction angle of 2θ is almost the same for both, Gc@PANI-ZnO-1 shows that this composite has characteristics representative of the three constituent materials.[38] Gc@PANI-ZnO-3 seems to have more dominant ZnO characteristics. The disappearance of the 2θ absorption peak at around 17°, 20°, and 29° of the Gc-PANI composite after the addition of ZnO indicates that the reduction process has occurred along with the synthesis of hybrid nanocomposites with hydrothermal techniques.[38] In the first preparation, Gc was soaked in an aniline monomer for 3 hours and continued with the addition of ammonium persulfate as an initiator of the polymerization process.[39] There are two forms of polyaniline emeraldine: a neutral emeraldine base. If the emeraldine base is protonated by acid on the imine nitrogen group, it turns into an emeraldine salt.[40] Protonation causes delocalization of the trapped diiminoquinone-diaminobenzene state.[41] Emeraldine base is the most desirable form of PANI because it remains stable at room temperature[42] the addition of acid to the emeraldine base forms an emeraldine salt, which makes PANI highly conductive.[43]

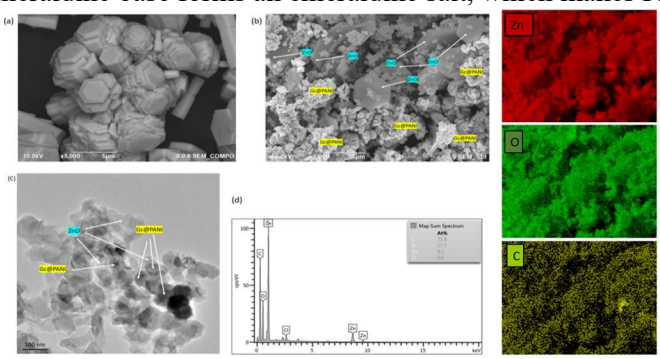

Fig.-4: SEM Image of (a) ZnO; (b) Gc@PANI-ZnO; (c) TEM Image of Gc@PANI-ZnO; (d) EDS Spectra of Gc@PANI-ZnO Composite

The morphology and structure of ZnO, Gc@PANI, and Gc@PANI-ZnO were characterized using SEM and TEM, which can be seen in Fig.-4. It can be seen that ZnO is agglomerated with a hexagonal-shaped surface; from the side of ZnO, it shows the shape of a ZnO-like pipe (Fig.-4a).[44] Gc@PANI appears to be distributed almost evenly, with particle sizes ranging from 197-199 nm. The Gc@PANI particles are attached to ZnO's surface (Figure 4). The TEM image of this Gc@PANI-ZnO hybrid composite clearly shows that PANI encases Gc in the form of a pipe and sticks to the surface of ZnO particles (Fig.-4c). An interaction between ZnO with Gc@PANI occurs by physisorption or is regulated by Van der Waals forces.[45] The strong link between ZnO and Gc@PANI affects the reuse of this photocatalyst.[46] The SEM-EDS of this composite material shows that this composite is composed of the elements Zn, C, and O. Encapsulation with PANI can improve the electrocatalytic properties of Gc. This encapsulation can also improve the compatibility of Gc with various types of electrocatalytic reactions. ZnO functions as a conductive material possessing energy levels appropriate for UV light absorption. The integration of Gc and ZnO minimizes fast photoinduced carrier recombination, thereby improving the photochemical process. PANI helps in more efficient charge transfer between ZnO and Gc.[47] As a result, Gc@PANI possesses a total area of 19.519 m^2/g, porosity capacity 0.990 cm^3/g, and thermal conductivity of $9.5x10^{-2}$ W/mK. As with the Gs@PANI-ZnO composite, this photocatalyst has a slightly lower total area measuring 18.706 m^2/g, a slightly larger adsorption volume reaching 0.991 cm^3/g, in addition to having thermal conductivity measuring 6.0 $x10^{-2}$ W/mK.

Photocatalytic Activity

The characteristics of the photocatalyst are significantly influenced by using spectral characteristics associated with the decrease in electron recombination and band gap energy. The photocatalytic performance regarding the Gc@PANI-ZnO hybrid composite was assessed using MB. The results of the

photodegradation of the catalyst on MB under a 500-watt halogen lamp are shown in Fig.-5. It shows that the maximum wavelength of MB is 665 nm. The decolourization of MB using the Gc@PANI-ZnO photocatalyst before irradiation and irradiation for 30 minutes shows the effectiveness of MB decolourization by reuse of the Gc@PANI-ZnO catalyst for the second and third times.

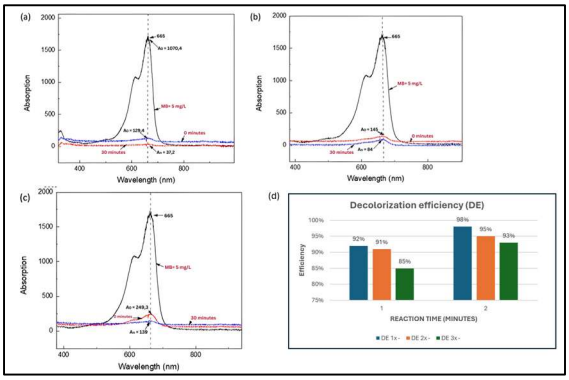

Fig.-5: Photocatalytic Activity and Decolorization Efficiency of the Hybrid Composite Gc@PANI-ZnO in (a) 1x; (b) 2x; (c) 3x Application Catalyst; (d) DE

A Particular light-responsive traits of Gc@PANI-ZnO were investigated via Optical absorbance spectroscopy, as depicted in Figure 5, and the effectiveness of the analysis was calculated based on the calculation results (Equation 1), showing that this catalyst can degrade colour in less than 30 minutes. Decolourization is associated with Gc's high BET surface area, providing more catalytically active centers for the photochemical reaction.[48] Gc also acts as an electron acceptor,[49] withdrawing electrons from UV-stimulated ZnO, which also prevents efficient recombination of electron-hole pairs.[50] Colour absorption becomes very efficient through the π-π conjugation structure in aromatic Gc.[51] Conversely, PANI also plays a significantly beneficial role by enhancing dye adsorption and capturing light to optimize the effectiveness of charge carrier separation and photogenerated voids.[52] When the photocatalyst is exposed to light, the light energy is absorbed by the catalyst, which causes an electron gap to form in it.[53] The pair of electron gaps formed interact with interacting water or oxygen molecules and drive an oxidation-reduction reaction, [54] in which electrons are delivered from holes to water or oxygen molecules, electron-accepting holes from water or oxygen molecules, producing hydroxyl radicals (OH..) and superoxide radicals (O_2.-).[55] The free radicals formed are highly reactive and can degrade MB by reducing the level of complexity so that it is more easily decomposed naturally in the environment.[56] According to Fig.-8, the reaction process involves: (i) A formation involving light-induced electron-hole pairs; (ii) the formation of O_2^- and OH^- species; (iii) Photochemical catalysis, including the photoinduced decomposition involving Organic hazardous materials and hydrogen (H_2) evolution reactions. It can be concluded that the improved photocatalytic performance of Gc@PANI-ZnO results from the synergistic effects of its strong visible light absorption capability, the establishment of a straightforward conductive pathway for enhanced conductivity through metal-based components, the efficient separation of photoinduced charge carriers, the higher interfacial •OH concentration on the material, and the increased surface-to-mass ratio of the substances. Singlet oxygen ($1O_2$) and superoxide radicals (O_2•) are recognized as key oxidative agents responsible for pollutant degradation.[57] The reaction step of photocatalytic degradation of MB was summarized (equations 3–8). The optical and photocatalytic activity of ZnO for pollutant degradation increases due to electrostatic interactions and covalent bonds.[58]

Decolorization Efficiency

Among the highly effective methods in activating catalytic breakdown is the UV process. The effectiveness of the UV treatment was assessed by the discoloration of a solution containing MB. That capability regarding the photocatalyst material to absorb UV light is a key factor influencing MB decolourization, as the dye degradation mechanism under UV irradiation relies on the generation concerning radicals by photogenerated electrons within the photocatalyst. The pace regarding photo-induced electrons rose as the power difference within the Gc@PANI-ZnO hybrid material reduced, while the recombination of (e^-/h^+) duos was minimized.

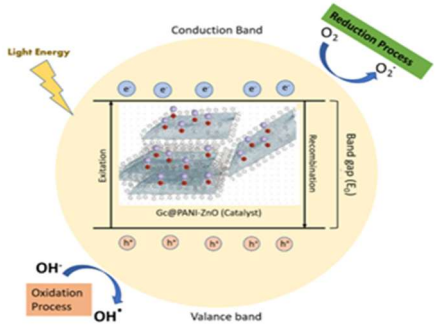

Fig.-6: Conceptual Schematic of the Photocatalytic Mechanism on the Gc@PANI-ZnO Catalyst

This suppression led to the production of a higher number of free radicals, thereby enhancing the MB photo-breakdown procedure. That photo-induced activity of the Gc@PANI-ZnO hybrid composite was remarkable. It is observed that when the catalyst is introduced into a 5 mg/L MB solution, stirred for 30 minutes, and subjected to ultrasonication for 5 minutes, MB undergoes 92% degradation without exposure to halogen lamp irradiation. The photocatalytic process was continued with irradiation for 30 minutes, and 98% degradation of MB occurred. Also, irradiation for 60 minutes obtained the same result of 98% (Table-2). For the reuse of the catalyst, the second use, there appears to be a slight decrease in effectiveness, namely 91% at 0 minutes (without a halogen lamp) and 95% after being given light for 30 minutes. Reusing the catalyst for the third time in the photocatalytic process showed a decrease in the effectiveness of MB decolourization to 85% before being exposed to light and 93% after being exposed to a halogen lamp for 30 minutes.

Table-2: Decolorization Efficiency (DE) Calculation Results, at λmax = 665 nm

Photodegradation Process		Gc@PANI-ZnO		
		MB 5 mg/L	0 minute	30 minutes
Adsorption	1x	1678.4	129.4	37.2
	2x	1678.4	145	84
	3x	1678.4	249.3	139
DE	1x	-	92%	98%
	2x	-	91%	95%
	3x	-	85%	93%

Reutilization of this catalyst in photocatalytic activity testing is essential for assessing its durability. Decolourization effectiveness of MB under halogen lamp exposure declined by 5% during the third reuse test after 30 minutes of illumination. The results of repeated reuse of this catalyst indicate that this Gc@PANI-ZnO nanocomposite hybrid photocatalyst can be used repeatedly with good and stable photocatalytic effectiveness. The relatively high photocatalytic activity of more than 90%, even when used repeatedly, indicates that this catalyst can absorb and degrade color during the photocatalytic process.

CONCLUSION

Gc was successfully extracted from sub-bituminous coal by the ultrasonication technique, and the Graphene@Polianilin-Zinc Oxide hybrid composite was successfully synthesized. The Gc is encapsulated by PANI to increase the Gc's stability and functionality in catalytic systems. The catalyst can absorb light and produce additional electron holes by adding ZnO, which is important for the photocatalytic process. The unique composition of the Gc nanocomposite hybrid catalyst, PANI, and ZnO, offers a photocatalytic activity of more than 90% and can be reusable for 3 cycles due to its excellent stability. These composites can be widely applied in various environmental and energy applications.

ACKNOWLEDGMENTS

Thanks to the Ministry of Education, Culture, and Research, Indonesia, for the funding with the granted number 125/E5/PG.02.00/PM.BARU/2024.

CONFLICT OF INTERESTS

The authors declare that there is no conflict of interest.

AUTHORS CONTRIBUTION

The present work is related to SDG-6: *Clean Water and Sanitation*. All the authors contributed significantly to this manuscript, participated in reviewing/editing and approved the final draft for publication. The research profile of the authors can be verified from their ORCID ids, given below:

V. Purwandari https://orcid.org/0000-0002-4263-5624
Marpongahtun https://orcid.org/0000-0003-1050-0431
Isnaeni https://orcid.org/0000-0001-5749-9891
M. Harahap https://orcid.org/0000-0001-9383-9769
Ronn Goei https://orcid.org/0000-0001-5958-4838
Henny Syapitri https://orcid.org/0000-0002-3257-053X

REFERENCES

1. E. O. Alegbe, and T. O. Uthman. *Heliyon,* **10**(13), e33646(2024), https://doi.org/10.1016/j.heliyon.2024.e33646
2. M. R. Repon, T. Islam, Paul, T. K., Jurkonienė, S., A. Haji, S. Shukhratov, and G. F. I. Toki, *Environmental Science and Pollution Research,* **31(35)**, 47552(2024), https://doi.org/10.1007/s11356-024-34424-1
3. A. K. Taloor, S. Sharma, S. Suryakiran, R. Sharma, and M. Sharma, *Current Opinion in Environmental Science & Health*, **39**, 100555(2024), https://doi.org/10.1016/j.coesh.2024.100555
4. A. S. Norfarhana, P. S. Khoo, R. A. Ilyas, N. H. Ab Hamid, H. A. Aisyah, M. N. F. Norrrahim, and P. K. Annamalai, *Journal of Polymers and the Environment*, **32(9)**, 4071(2024), https://doi.org/10.1007/s10924-024-03227-3
5. I. Tyagi, V. Kumar, and K. Tyagi, *Water, The Environment, and the Sustainable Development Goals*, pp. 35-66 (2024), https://doi.org/10.1016/B978-0-443-15354-9.00008-6
6. S. Jan, Mishra, A. K. Bhat, M. A, Bhat, and A. T. Jan, *Environmental Science and Pollution Research*, **30(53)**, 113242(2023), https://doi.org/10.1007/s11356-023-30302-4
7. K. Nagaraj, S. Radha, C. G. Deepa, K. Raja, V. Umapathy, N. P. Badgujar, and C. Uthra, *Next Research*, **2(1)**, 100180(2025), https://doi.org/10.1016/j.nexres.2025.100180
8. N. M. Chauke, R. L. Mohlala, S. Ngqoloda, and M. C. Raphulu, *Frontiers in Chemical Engineering*, **6**, 1356021(2024), https://doi.org/10.3389/fceng.2024.1356021
9. T. Hisatomi, T. Yamada, H. Nishiyama, T. Takata, and K. Domen, *Nature Reviews Materials*, 1-14 (2025), https://doi.org/10.1038/s41578-025-00823-0
10. E. Galvagno, E. Tartaglia, M. Stratigaki, C. Tossi, L. Marasco, F. Menegazzo, and M. Moglianetti, *Advanced Functional Materials*, **34(13)**, 2313043(2024), https://doi.org/10.1002/adfm.202313043
11. N. K. Prasad, K. C. B. Naidu, and D. Baba Basha, *Crystals*, **14(9)**, 781(2024), https://doi.org/10.3390/cryst14090781
12. N. S. N. Hasnan, N. A. Nordin, and M. A. Mohamed, *Journal of Materials Chemistry A*, **12**, 27892(2024), https://doi.org/10.1039/D4TA03977G
13. P. Hait, R. Mehta, and S. Basu, *New Journal of Chemistry,* (2025), https://doi.org/ 10.1039/D5NJ02247A
14. Y. Li, F. Zhang, K. Xu, Z. Yang, and Z. Dong, *Colloids and Surfaces A: Physicochemical and Engineering Aspects*, **700**, 134803(2024), https://doi.org/10.1016/j.colsurfa.2024.134803
15. M. Harun-Ur-Rashid, K. Pal, and A. B. Imran, *Topics in Catalysis*, **67(1)**, 17(2024), https://doi.org/10.1007/s11244-023-01809-4

16. H. Ehtesabi, *Nanomaterials in Environmental Analysis*, pp. 109-127, Elsevier(2024), https://doi.org/10.1016/B978-0-12-820643-0.00008-0
17. T. Ramachandran, N. Roy, H. H. Hegazy, I. S. Yahia, Y. A. Kumar, M. Moniruzzaman, and S. W. Joo, *Journal of Alloys and Compounds*, **1010**, 177248(2025), https://doi.org/10.1016/j.jallcom.2024.177248
18. A. Khan, S. N. Sapakal, and A. Kadam, *Graphene and 2D Materials*, **9(1)**, 101(2024), https://doi.org/10.1007/s41127-024-00072-y
19. S. A. Anushya, and A. Philominal, *Diamond and Related Materials*, **149**, 111592(2024), https://doi.org/10.1016/j.diamond.2024.111592
20. A. Umar, F. Ahmed, N. Ullah, S. A. Ansari, S. Hussain, A. A. Ibrahim, S. Baskoutas, *Electrochimica Acta*, **479**, 143743(2024), https://doi.org/10.1016/j.electacta.2023.143743
21. W. Zhao, M. Cui, Y. Zhou, Y. Liu, R. Liang, Q. Ou, and S. Zhang, *Journal of Energy Storage*, **99**, 113471(2024), https://doi.org/10.1016/j.est.2024.113471
22. I. Ahma d, M. S. Athar, M. Muneer, H. M.Altass, R. Felemban, and S. A. Ahmed, *Nanoscale*, **17(7)**, 3822(2025), https://doi.org/ 10.1039/D4NR03681F
23. S. A. Mousa, D. A. Wissa, H. H. Hassan, A. A. Ebnalwaled, and S. A. Khairy, *Scientific Reports*, **14(1)**, 16713(2024), https://doi.org/10.1038/s41598-024-66975-1
24. Y. Su, Y. Wu, D. Cai, D. Zou, and Y. Li, *Separation and Purification Technology*, **354**, 129394(2025), https://doi.org/10.1016/j.seppur.2024.129394
25. P. Rana, V. Soni, R. Kumar, A. Chawla, A. A. P. Khan, P. Singh, and K. A. Alzahrani, *Fuel*, **386**, 134286(2025), https://doi.org/10.1016/j.fuel.2025.134286
26. Y. Yang, X. Liu, D. He, and F. Jin, *Nano-Micro Letters*, **17(1)**, 216(2025), https://doi.org/10.1007/s40820-025-01711-6
27. X. Ning, A. Hao, R. Chen, M. F. Khan, and D. Jia, *Carbon*, **218**, 118772(2024), https://doi.org/10.1016/j.carbon.2023.118772
28. F. K. Muhammad, and J. C. Arulanandam, *Zeitschrift für Physikalische Chemie*, **239(6)**, 839(2025), https://doi.org/10.1016/j.ceramint.2024.01.086
29. M. Zhang, X. Sun, C. Wang, Y. Wang, Z. Tan, J. Li, and B. Xi, *Materials Chemistry and Physics*, **278**, 125697(2022), https://doi.org/10.1016/j.matchemphys.2022.125697
30. S. Fan, Q. Yang, G. Yin, X. Qi, Y. Feng, J. Ding, and X. Gong, *Small*, **20(29)**, 2311978(2024), https://doi.org/10.1002/smll.202311978
31. E. Özgenç, M. K. Çoruh, E. Keleş Özgenç, A. H. Dönmez, and G. Y. Töre, *Handbook of Nanofillers*, pp. 999-1034, Springer Nature (2025), https://doi.org/10.1007/978-981-96-2407-2_56
32. V. Losetty, S. K. Lakkaboyana, H. Y. Chappidi, K. Venkateswarlu, H. Trilaksana, J. R. Koduru, and S. Knani, *Journal of Inorganic and Organometallic Polymers and Materials*, 1-33, (2025), https://doi.org/10.1007/s10904-025-03707-6
33. J. A. Sarkar, M. S. Siddiqui, and M. Aslam, *Scientific Reports*, **15(1)**, 31505(2025), https://doi.org/10.1038/s41598-025-99502-x
34. S. A. Disha, M. S. Hossain, M. L. Habib, and S. Ahmed, *Results in Materials*, **21**, 100496(2024), https://doi.org/10.1016/j.rinma.2023.100496
35. M. Soltani, N. Ahmadzadeh, S. Rajabi, N. Besharati, N. Khatamian, and M. Homayouni Tabrizi, *Scientific Reports*, **15(1)**, 8494(2025), https://doi.org/10.1038/s41598-024-81604-7
36. S. W. Suciyati, P. Manurung, J. Junaidi, and R. Situmeang, *Indonesian Journal of Chemistry*, **24(1)**, 125(2024), https://doi.org/10.22146/ijc.84796

37. N. Soni, N. Dhariwal, P. Yadav, and V. Kumar, *Journal of Materials Science: Materials in Electronics*, **35(22)**, 1521(2024), https://doi.org/10.1007/s10854-024-13281-1
38. M. Beygisangchin, S. A. Rashid, S. Shafie, and S. K Kamarudin. *Research on Chemical Intermediates*, **50(8)**, 3869(2024), https://doi.org/10.1007/s11164-024-05340-3
39. U. Baig, A. Waheed, J. Usman, and I. H. Aljundi, *ACS Applied Materials & Interfaces*, **16(26)**, 33504(2024), https://doi.org/10.1021/acsami.4c05543
40. E. Wongrat, I. Moonmuang, N. Chanlek, N. Hongsith, S. Pramchu, and S. Choopun, *Sensors and Actuators B: Chemical*, **441**, 137981, (2025), https://doi.org/10.1016/j.snb.2025.137981
41. R. Farina, S. Scalese, D. Corso, G. E. Capuano, G. A. Screpis, M. A. Coniglio, and S. Libertino, *Molecules*, **29(13)**, 3028(2024), https://doi.org/10.3390/molecules29133028
42. G. Sasikanth, B. V. R. S. Subramanyam, and T. P. Radhakrishnan, *The Journal of Physical Chemistry C*, **128(26)**, 10818(2024), https://doi.org/10.1021/acs.jpcc.4c02578
43. C. D. Gandhi, and P. Sappidi, *Journal of Molecular Liquids*, **402**, 124748(2024), https://doi.org/10.1016/j.molliq.2024.124748
44. V. N. Hegde, *Journal of Science: Advanced Materials and Devices*, **9(3)**, 100733(2024), https://doi.org/10.1016/j.jsamd.2024.100733
45. Z. Li, K. Guo, C. Yin, Y. Li, and S. F. Mertens, *Molecules*, **30(4)**, 926(2025), https://doi.org/10.3390/molecules30040926
46. P. Lawtae, S. Meephon, V. Dokmai, R. Methaapanon, and V. Pavarajarn, *Journal of Materials Chemistry A*, **13(17)**, 12327(2025), https://doi.org/10.1039/D5TA00833F
47. S. Simon, and P. B. Sreeja, *Energy Storage*, **6(8)**, e70101(2024), https://doi.org/10.1002/est2.70101
48. S. K. Afridi, and K. Umar, *Catalysis Letters*, **155(5)**, 167(2025), https://doi.org/10.1007/s10562-025-05000-0
49. M. Mansouri, C. Díaz, and F. Martín, *Communications Materials*, **5(1)**, 117(2024), https://doi.org/10.1038/s43246-024-00549-6
50. M. C. Silva, S. Castro-Lopes, A. G. Jerônimo, R. Barbosa, A. Lins, P. Trigueiro, and R. R. Peña-Garcia, *Molecules*, **29(2)**, 391(2024), https://doi.org/10.3390/molecules29020391
51. X. Huang, W. Ye, J. Zhuang, C. Hu, H. Dong, B. Lei, and Y. Liu, *ACS Sustainable Chemistry & Engineering*, **12(28)**, 10399(2024), https://doi.org/10.1021/acssuschemeng.4c01739
52. M. A. Shahat, M. A. Ibrahim, A. Ghitas, and H. A. Ezzat, *Journal of Molecular Structure*, **1327**, 141220(2025), https://doi.org/10.1016/j.molstruc.2024.141220
53. O. F. Aldosari, *Catalysis Reviews*, 1-38, (2025), https://doi.org/10.1080/01614940.2024.2446476
54. A. Yu, and Y. Yang, *Angewandte Chemie*, **137(16)**, e202424161(2025), https://doi.org/10.1002/ange.202424161
55. W. Chi, J. Wu, Y. Dong, J. Wu, and Y. Zhu, *Angewandte Chemie International Edition*, e202508690, (2025), https://doi.org/10.1002/anie.202508690
56. Y. Chen, S. Xu, C. Fang Wen, H. Zhang, T. Zhang, F. Lv, and Z. Bian, *Chemistry–A European Journal*, **30(29)**, e202400001(2024), https://doi.org/10.1002/chem.202400001
57. M. Elsafi, Y. C. Ho, B. H. Guan, W. H. Leong, and N. M. Rashid, *Biomass Conversion and Biorefinery*, **15**, 17951(2025), https://doi.org/10.1007/s13399-024-06441-0
58. M. A. Ahmed, M. A. Ahmed, and A. A. Mohamed, *Optical Materials*, **151**, 115339(2024), https://doi.org/10.1016/j.optmat.2024.115339

[RJC-9288/2025]